Supporting Information

# Steering epitaxial alignment of Au, Pd, and AuPd nanowire arrays by atom flux change

Youngdong Yoo,[†] Kwanyong Seo,[†] Sol Han,[†] Kumar S. K. Varadwaj,[†] Hyun You Kim,[‡] Ji Hoon Ryu,[‡] Hyuck Mo Lee,[‡] Jae Pyoung Ahn,[§] Hyotcherl Ihee,[†] and Bongsoo Kim*[,†]

*Department of Chemistry, KAIST, Daejeon 305-701, Korea, Department of Materials Science and Engineering, KAIST, Daejeon 305-701, Korea, Nano-Material Research Center, KIST, Seoul 136-791, Korea.*

To whom correspondence should be addressed. E-mail: bonsoo@kaist.ac.kr

[†] Department of Chemistry, KAIST, Daejeon 305-701, Korea

[‡] Department of Materials Science and Engineering, KAIST, Daejeon 305-701, Korea

[§] Nano-Materials Research Center, KIST, Seoul 136-791, Korea

## Materials and Methods

**Synthesis.** Au, Pd, and AuPd nanowires (NWs) were synthesized in a horizontal hot-wall single-zone furnace with a 1 in. diameter inner quartz tube. Ar gas flowed at a rate of 100 sccm, maintaining the chamber pressure at 5 ~ 15 Torr. The metal slug (Au and Pd), which was placed in an alumina boat at the center of a heating zone, was heated and the vapor was transported to the lower temperature region by carrier gas, where metal NWs were grown on sapphire substrates. The distance from the center of the heating zone to the center of the substrate was 5.3 cm at the source temperature of 1,100 °C and 8.5 cm at 1,300 °C. The temperature of the substrates was maintained at 1,000 °C for both experiments. For all experiments, the size of substrate was $4 \times 4$ mm$^2$ and the reaction time was between 5 min and 30 min.

**Characterization.** SEM images were taken on a Phillips XL30S. Samples were coated with gold in the SEM observation. TEM and HRTEM images and SAED patterns were taken on a TECNAI F30 TEM. Cross-sectional TEM specimens were prepared by a dual-beam focused ion beam (FEI Nova 600 NanoLab) equipped with a nanomanipulator (Kleindick MM3A). XRD patterns of the specimen were recorded on a Rigaku D/max-RC (12 kW) diffractometer.

## Supplementary Figures

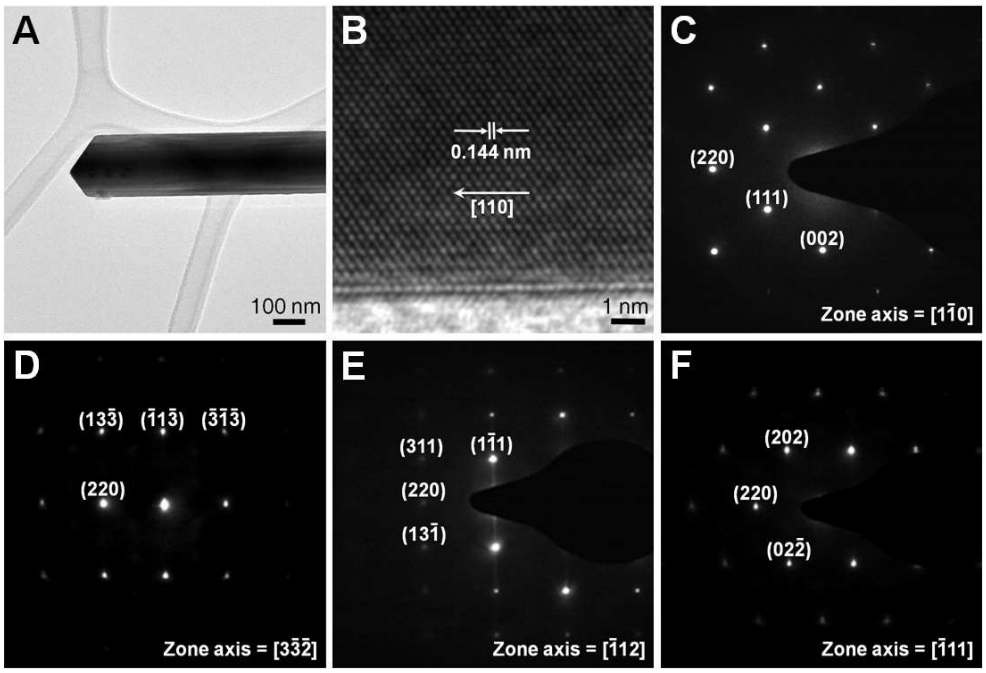


**Figure S1.** TEM images and SAED patterns of a Au NW. (A) Low-resolution TEM image of the Au NW. The angle between two facets of the NW tip is measured to be 109.5°, which is consistent with the angle between two {111} facets. (B) High-resolution TEM image of the Au NW. The NW is single crystalline with a [110] growth direction and does not have twins or defects. (C to F) SAED patterns observed at various zone axes by rotating along the long axis of the NW. All of the spot patterns can be assigned to the fcc Au structure, further confirming the single crystalline nature of the NWs.

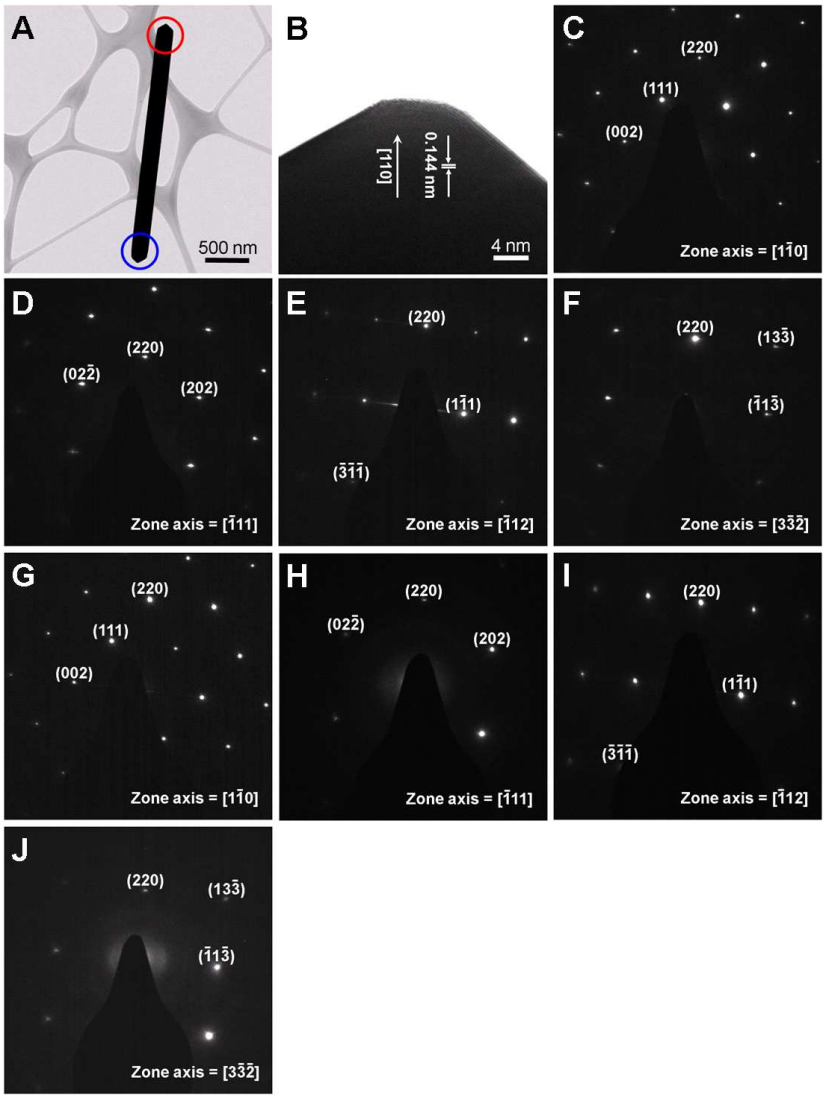


**Figure S2.** TEM images and SAED patterns of the tip and the root parts of a Au NW. (A) Low-resolution TEM image of a Au NW. (B) High resolution TEM image of a Au NW tip. (C to F) SAED patterns of a Au NW tip indicated by a red circle in (A). (G to J) SAED patterns of a Au NW tip indicated by a blue circle in (A). We took the SAED pattern at the beginning and the end of a NW. The patterns show that they are all single-crystalline. The red circle and the blue circle represent the tip and the root parts of a Au NW. It is likely that the root part became acute when the NW was detached from the substrate by a nanomanipulator.

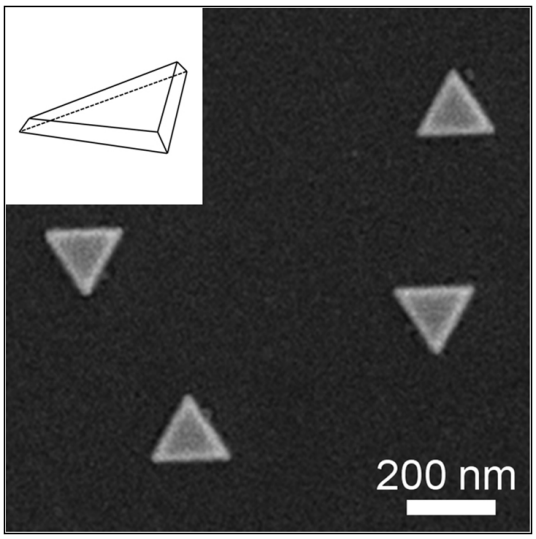


**Figure S3.** Magnified top-view SEM image of triangular plates grown on a c-cut sapphire substrate at the source temperature of 1,300˚C (high flux condition) as seen in Figure 1e. The inset is a three-dimensional schematic. Generally, more diverse nanostructures are observed at a high flux condition, which may be ascribed to the higher surface diffusion. The observed triangular plates are truncated tetrahedra. In the high flux condition, surface diffusion plays an important role to the nanostructure growth. The angle between the seed face and the substrate (reentrant angle) is 90˚ for a half-octahedral seed, while that for this truncated tetrahedron is 109.47˚. It is more advantageous to have a smaller reentrant angle for the growth of nanostructure by the surface diffusion (J. Am. Ceram. Soc. 83, 385 (2000)). Since the half-octahedral seed grows faster than the truncated tetrahedral seed and the crystal growth occurs competitively, the triangular plates do not grow very large. Also the growth would make a larger plate, not leading to a NW, because the three growth directions are all equivalent.

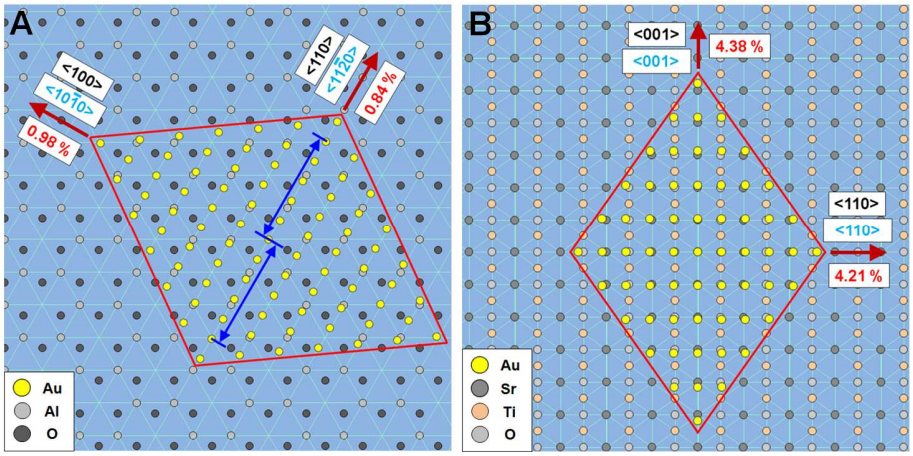


**Figure. S4.** The lattice mismatch of the half-octahedral Au seed on a c-cut sapphire and an Nb-doped $SrTiO_3$ (110) substrate. (A) In the case of (110) Au // (0001) sapphire, the lattice mismatch between Au and sapphire is 0.98 % along the Au <100> direction. While the lattice mismatch is 19.01 % along the Au <110> direction, the mismatch becomes only 0.84 %, when we consider a larger domain, where 5 layers of Au are matched with 3 layers of sapphire (refer to the model of domain matching epitaxy: J. Narayan and B. C. Larson, J. Appl. Phys. 93, 278 (2003)). (B) In the case of (110) Au // (110) Nb-doped $SrTiO_3$ substrates the lattice mismatch between Au and $SrTiO_3$ is 4.38 % along the Au <001> direction and 4.21 % along the Au <110> direction. Nb-doped $SrTiO_3$ (110) substrates have a relatively good lattice match with the Au (110) plane because of similar arrangements of atoms.

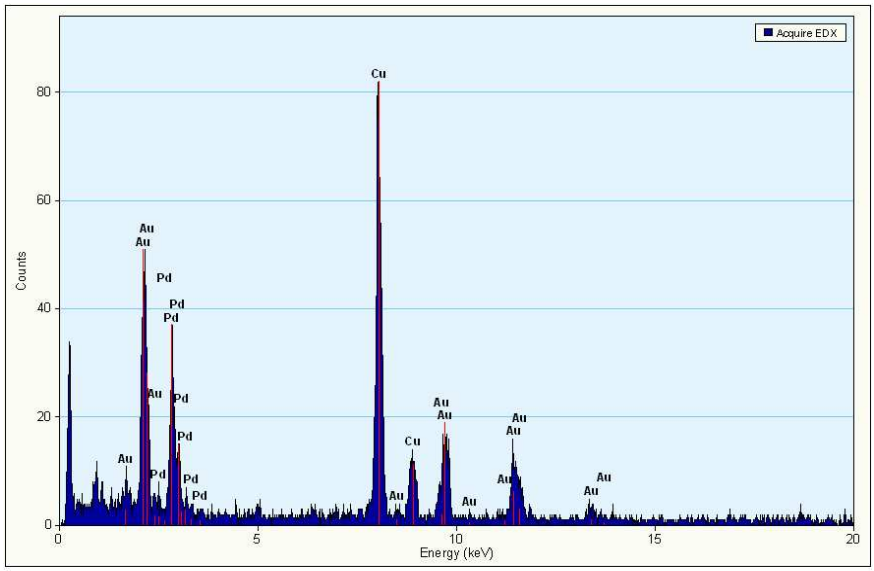


| Element | Weight % | Atomic % | Uncertainty % | Correction | k-Factor |
|---|---|---|---|---|---|
| Au(L) | 71.249 | 57.241 | 2.801 | 0.753 | 5.950 |
| Pd(L) | 28.750 | 42.758 | 1.431 | 0.937 | 2.804 |

**Figure S5.** TEM-EDS analysis of a single AuPd alloy NW. Detailed analysis of several AuPd alloy NWs dispersed on the carbon coated copper TEM grid confirms approximately 1:1 atomic ratio of Au and Pd.

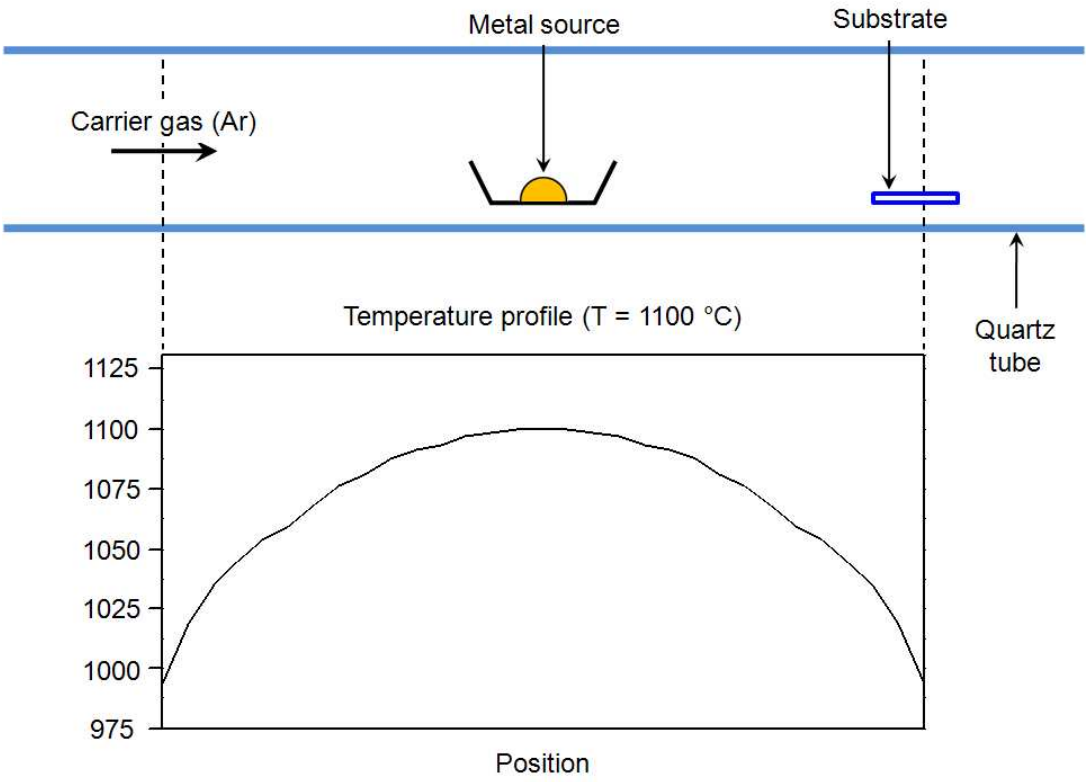


**Figure S6.** Experimental set-up used for synthesis of vertical Au, Pd, AuPd NWs. Shown below the furnace is the temperature profile, indicating that the centre of the heating zone is maintained at 1100 °C, whereas the substrates are at 1000 °C.

## Molecular Dynamics Simulations

The temperature for MD simulation is set to 800 K because of the small size of the seed employed in the calculation. Surface melting of the seed was observed because of the melting temperature lowering on the size reduction when the simulation temperature was set at 1,270 K of the real experiments. 800 K is the optimized temperature for the stability of the seed against melting and the diffusion of Au atoms and clusters on the substrate.

We took small size of seed (1 – 2 nm) for our MD simulations for computational speed. In current level of MD simulation, dealing with a system larger than 10 nm is too much time-consuming. What we intended to find by simulation was to see if the Au atoms adsorbed on the top face would diffuse down and contribute significantly to the horizontal growth and the Au atoms approaching the seed by surface diffusion would climb up to the top face and contribute to the vertical growth. (This will confirm if vertical growth occurs when vertical flux is dominant and horizontal growth occurs when horizontal flux is dominant.)

Since we do not want the small size of seed to alter the growth mechanism of a NW we proposed here, the size of seed employed in the calculation is carefully optimized not to hinder the adsorption and diffusion of Au clusters and atoms on the surface and edges of the Au seed. The initial seed structure is fixed and the colliding of the Au atoms from the air is not considered. Considering these limitations in the simulation, the Au atom diffusion behavior and NW growing mechanism can be considered as meaningful, but quantitative prediction does not seem possible.

The simulation provides similar results to the experiment because the simulation used an initially formed seed of a fixed structure. The important steps in this seed-initiated NW growth are (i) epitaxial formation of the seed on the substrate (ii) material flux direction (iii) the lattice match between the substrate and the NWs. For the vertical NW growth, it is observed in the MD simulation that the newly added Au atoms on the top face of the seed rarely diffuse down to the side face and reach to the graphite substrate. Since there is no interaction between the substrate and the added Au atoms, the

simulation result is quite the same with the experiments in spite of employing the graphite substrate. For the horizontal growth, however, the Au atoms approach the seed via the graphite surface that does not have good lattice match with Au NWs. The simulation shows that the crystal structure of newly formed Au layers on the side face of a Au seed starts to deviate from the fcc structure when the NW grows by more than several layers. The graphite substrate provides good mobility for Au atoms and clusters similarly to the sapphire substrate, but does not provide a good lattice match and thus would not allow epitaxial horizontal growth of Au NW. If the simulation employs a sapphire substrate, which has a more complicated structure but much better lattice match with Au crystals than graphite, long Au NW growth as seen in the experiment would be observed from the MD simulation.

## Supplementary Movie Legends

### Movie S1

Simulation of the growth process of a vertical Au NW from a half-octahedral seed by direct impingement of Au atoms as seen from the side. When Au atoms are supplied to the half-octahedral seed by direct impingement, the seed grows vertically.

### Movie S2

Simulation of the growth process of a horizontal Au NW from a half-octahedral seed by surface diffusion of Au atoms as seen from the top. When the Au atoms are approaching the half-octahedral seed by surface diffusion, the seed grows horizontally.